sciendo

DOI: 10.2478/fv-2024-0001

FOLIA VETERINARIA, 68, 1: 1—14, 2024

HISTOMORPHOLOGICAL INVESTIGATION OF THE EYE OF THE TREE SQUIRREL: A PRELIMINARY STUDY

James O. Olopade, Olanrewaju I. Fatola, Taidinda T. Gilbert, Oluwabusayo R. Folarin, Adedunsola A. Obasa, Jude I. Abeje, Munachimso K. Njasi, Ejiro O. Ighorodje, Chizubelu I. Omile, Kehinde I. Adedokun

Neuroscience Unit, Department of Veterinary Anatomy, Faculty of Veterinary Medicine, University of Ibadan, Ibadan Nigeria

fatolan@yahoo.com

ABSTRACT

Squirrels are diurnal rodents with high visual acuity including unique properties well-suited for their natural environment. This study was conducted to explore some ocular microscopic features of tree-harbouring squirrels in the University of Ibadan, Ibadan, Nigeria. Two male squirrels were cage-trapped within the University premises. Light microscopic analysis was carried on paraffin-embedded eye samples harvested from the animals. The densely compacted stromal fibres, 351 ± 52.5 µm thick, formed the thickest part of the cornea, and the basement membrane of the corneal epithelium, 63.8 ± 13.0 µm thick, was notably positive with Periodic Acid Schiff (PAS) stain. Strong pigmentation was present at the choroid as well as the iridal and ciliary epithelia. The multiple layering of the retinal structure exhibited densely packed ganglion cells at the ganglion cell layer which together with the nerve fibre layer was observed to be thinnest at the more peripheral portion but becomes thicker towards the optic disc. Strongly positive glia fibrillary acidic protein (GFAP+) cells with their abundant fibrous processes were demonstrated immunohistochemically at the retinal nerve fibre layer and the optic nerve. Histological features of the retinal cellular components of the tree squirrels investigated has thus highlighted the structural adaptation of these animal species to their environmental arboreal habitat and diurnal lifestyle. Findings from this study, while further noted to be similar to that in human, showed that African tree squirrels represent promising rodent model for human retinal/ocular research.

Key words: diurnal lifestyle; histology; ocular structures; retinal ganglion cells; tree squirrel

INTRODUCTION

Survival of an animal in a given habitat is a function of how well such animal can adapt its lifestyle to the environment which in turn facilitates structural adjustments [27]. In this vein, research works have shown that the eye structural make-up is influenced by the natural environment as well as mode of life. This structural adaptation is observed as morphological variations, particularly in the retina, the photosensitive aspect of the eye [15, 54].

Squirrels are mostly diurnal mammals [51, 88] belonging to the *Sciuridae* rodent family [77]. These animal

species are beneficial in the food chain as seed dispersal/pollination agents [45] and protein sources [16, 31]. They are also of public health importance as pests and disease vectors as well as models for research in the scientific field [82]. Over 270 species and 60 genera of flying, ground and tree squirrels are found in a wide range of habitat across the globe. Among the 11 squirrel species reportedly distributed throughout Nigeria are Thomas's Rope (*Funisciurus anerythrus* Thomas, 1890) and Gambian Sun (*Heliosciurus Gambianus* Ogilby, 1835) tree squirrels [45] mainly sourced for meat consumption as well as for therapeutic use [72].

The feeding strategy of squirrels having high visual acuity [41, 48, 51, 81] is herbivorous primarily [52]. The tree living squirrels also scout for what to eat on the ground and their reliance for sharp vision is critical for them to explore their habitat as they search for food while steering clear of predators [28, 30, 78]. Moreover, arboreal rodents like the Gambian Sun and Thomas's Rope squirrels staying mostly in trees, indicates their need for accurate vision to navigate the trees as they jump from branches to branches [52, 78]. Campi and Krubitzer [12] reported that the greater reliance on vision in the arboreal squirrels compared with the terrestrial squirrels is reflected in the larger proportion of two of the cortical sheets in the brain. Vision scientists have further established that the retinal ganglion cells of these rodents project to highly organized visual brain areas which have been adequately investigated in ground squirrels but less researched into in the tree squirrels [84].

Additionally, these mammalian species are not among the extensively-studied rodents within the sub-Saharan African region as documented data are preliminary findings in most cases [39, 65]. In this respect, in Nigeria, squirrel research works are limited to parasitic worm [66] as well as organ morphology investigations [4, 19, 20, 38] while data regarding squirrel's eyes are to the best of our knowledge yet to be documented.

Hence, this study is aimed at presenting preliminary histomorphometrics and histomorphology eye structures in tree squirrels (Thomas's Rope and Gambian Sun tree squirrels) within the University of Ibadan, Ibadan, Nigeria which could serve as a baseline data useful in biomedical research and enrich an understanding regarding the structural adaptation of the eyes of the African tree squirrel to its habitat.

MATERIALS AND METHODS

Experimental animals

Two male squirrels were used for this study and the eyeballs of the animals (2 each) were analysed. The animals (1 Thomas's Rope squirrel (TRS) (166.6 g) and 1 Gambian Sun squirrel (GSS) (244.9 g) were cage-trapped at the University of Ibadan located at longitude $7^0$23'47"N and latitude $3^0$55'0"E south-west of Nigeria in Ibadan city. The two tree squirrels investigated in this work were among the animal species originally ratified by the institution's Animal Care and Use Research Ethics Committee (Assigned Number: *UI-ACUREC/099-0921/22*) regarding an ongoing arbovirus surveillance project of Humboldt Research Hub for Zoonotic Arbovirus Diseases (HRH-ZAD) being executed at the University of Ibadan, Ibadan, Nigeria.

Euthanasia was carried out using an overdose of a combination of xylazine (10 $mg.kg^{-1}$ b.w.) and ketamine (100 $mg.kg^{-1}$ b.w.) administered intramuscularly, death being confirmed by absence of heart rate, and following careful eye enucleation [35], the eyes were fixed in Davidson's fluid [2] for 24 hours and then 10 % neutral buffered formalin (NBF). Orientation of the eyeball was achieved with the superior rectus muscle as point of reference for dorsal positioning (Fig. 1A), in addition to making an easily-recognizable cut within dorsal cornea region, midway between the two canthi [79]. A small incision was then made on both the lateral (temporal canthus) and medial (nasal canthus) sides to ensure proper fixation. Each eyeball was thereafter trimmed dorso-ventrally (sagittaly) for processing to paraffin blocks.

Light microscopy

Five µm slide sections were produced from 4 eyeballs in total for routine haematoxylin and eosin (H&E) [5], Periodic Acid Schiff (PAS) [49] staining as well as immunohistochemistry [40] using anti Glial Fibrillary Acidic Protein (GFAP) (2A5) mouse monoclonal primary antibody 1:2000 (Abcam, Boston, USA). Briefly, antigen retrieval was done by microwave heating in 10 mM citrate buffer for 25 minutes, with subsequent peroxidase quenching in 3 % H_2O_2/methanol. All the sections were blocked in 2 % skimmed milk overnight and probed with anti-GFAP mouse monoclonal antibody for 16 hours at 4 °C. Detection of bound antibody was done using appropriate HRP-con-

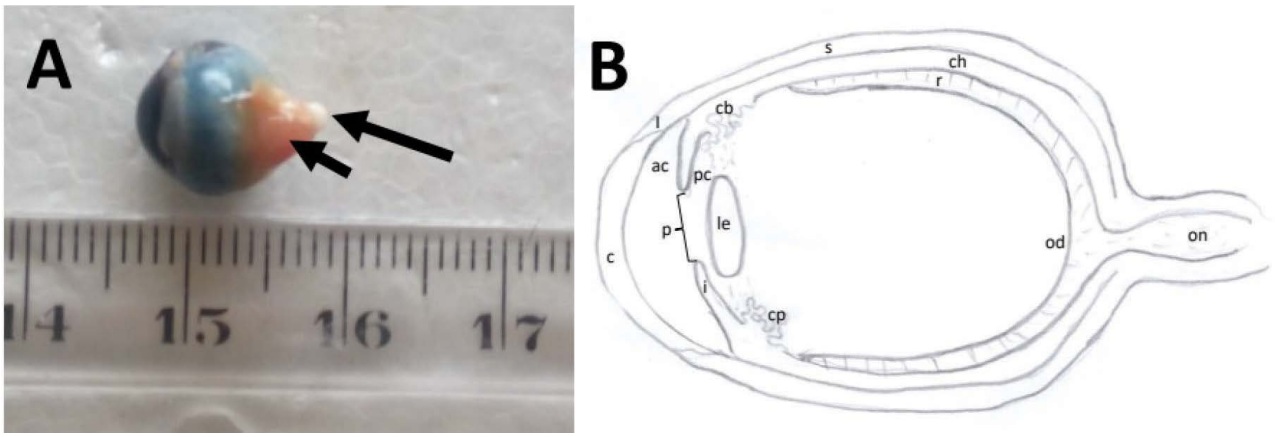

Fig. 1. TRS/GSS eyeball.
(A) Orientation of the eyeball using the superior rectus muscle (short-tailed arrow) as landmark for dorsal positioning, optic nerve (long-tailed arrow); (B) Schematic diagram of the eye structures; c – cornea; s – sclera; l – limbus; ac – anterior chamber; pc – posterior chamber; p – pupil; i – iris; cb – ciliary body; ch – choroid; r– retina; od – optic disc; on – optic nerve (diagram not drawn to scale).

jugated secondary antibodies in VECTASTAIN kit (Vector Labs) according to the manufacturer's protocol. The reaction product was enhanced with DAB for 6–10 minutes, with subsequent dehydration in ethanol and mounting on slides. Photomicrographs were obtained with the help of a light microscope (Leica DM500) fitted with digital camera (Leica ICC50 E) (Leica Microsystems, Wetzlar, Germany). Images were captured at x10 and x40 objective lens and histomorphometry performed using Motic Images Plus 2.0 software (Motic China Group Co. Ltd., Kowloon, Hong Kong). The measurements were taken especially for retina at five sites about midway from the peripheral region of retina (beginning of pars ciliaris retinae) to the optic nerve head [90], as a result of non-uniform thickness of the retinal layers. A total of fifteen measurements per eye was recorded (Table 1).

Statistical analysis

The data curation was done using GraphPad prism version 8 (GraphPad Software, San Diego, California, USA). Relative thicknesses of the corneal and retinal layers were recorded and the measurements documented as the Mean ± Standard Error of the Means (SEM).

The two squirrel strains were analysed together because i) no gross differences were observed between both strains, ii) in order to find similarities that differentiate diurnal squirrels from other nocturnal rodents.

Ethical approval

The four tree squirrels investigated in this work were among the animal species originally ratified by the institution's Animal Care and Use Research Ethics Committee (Assigned Number: *UI-ACUREC/099-0921/22*) regarding an ongoing arbovirus surveillance project of Humboldt Research Hub for Zoonotic Arbovirus Diseases (HRH-ZAD) being executed at the University of Ibadan, Ibadan, Nigeria.

RESULTS

Histology

The eye generally is bounded by a wall of three layers: outer fibrous tunic; middle vascular tunic; inner retinal/photosensitive layer. The outer tunic is pierced by the optic nerve connecting the eye to the brain (Fig. 1).

Some structures of the eyes of TRS and GSS tree squirrels, as illustrated in Fig. 1B, were examined histologically and the findings include:

Sclera

The sclera was composed of (from outermost layer to innermost layer): (1) episclera lamina – dense fibrous connective tissue; (2) proper substance of sclera – consisting collagen fibres, network of elastic fibres, and blood vessels (Fig. 2).

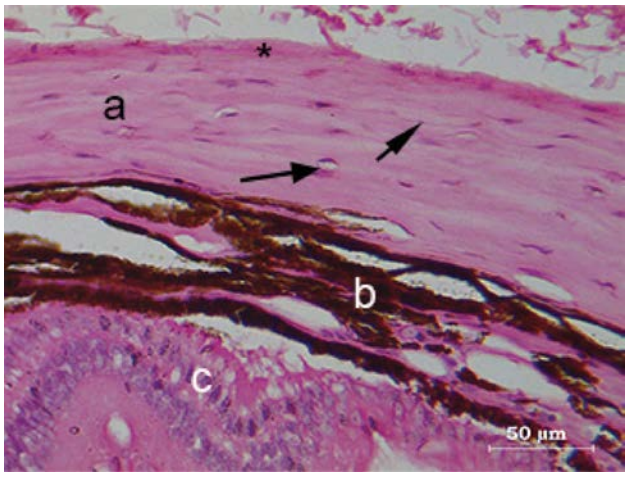

Fig. 2. Photomicrograph of the sclera of tree squirrel. Fibrous connective tissue of sclera (a) with dense episclera (*), network of elastic fibres (short-tailed arrow), blood vessels (long-tailed arrow) and underlying choroid (b) and retina (c). Haematoxylin-Eosin stain.

Cornea

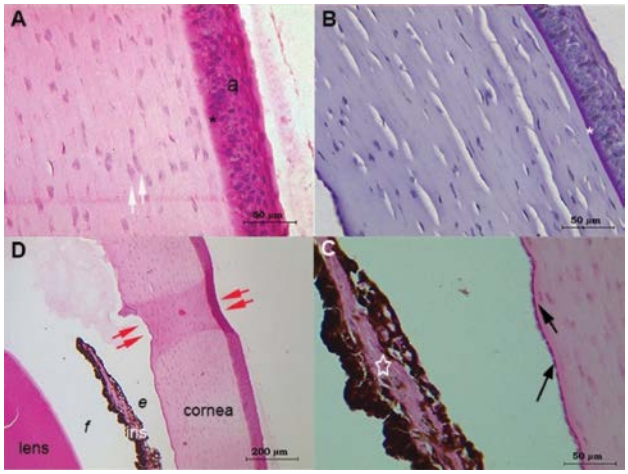

Fig. 3. Photomicrograph of the cornea of tree squirrel. (A) Nonkeratinized stratified squamous epithelium (a) separated by basement membrane (*) from parallel arranged collagenous fibres (white arrows). (B) Basement membrane (*), strongly positive for Periodic Acid Schiff stain, of basal columnar epithelial cell layer. (C) Corneal stroma separated by slightly more eosinophilic Descemet's membrane (short-tailed arrow) from single layered posterior epithelium (long-tailed arrow), iris (white star). (D) Iris divides eye cavity filled with aqueous humour into the anterior (e) and posterior (f) chambers, processing artefacts (double red arrows). Haematoxylin-Eosin stain, A, C; Periodic Acid Schiff, B.

The outer or anterior covering (corneal epithelium) of the avascular cornea was nonkeratinized and comprises stratified squamous epithelium of about 6–10 layers of cells. The corneal epithelial cells became more flattened towards the apical border (Fig. 3A) while at the basal border, more prominent basement membrane borders the corneal epithelium and the proper substance of the cornea (stroma) (Fig. 3B). Tightly layered collagenous fibrils made up bulk of the stroma, the thickest part of cornea. These fibrils were arranged in a parallel fashion. The stroma was separated from the posterior corneal epithelium by the Descemet's membrane. The Descemet's membrane was a thin layer of slightly more eosinophilic membrane while the posterior epithelium, made up of squamous cells, lining the posterior boundary of cornea was single layered (Fig. 3B, C). The aqueous-filled cavity bounded between the cornea and lens was demarcated into the anterior and posterior chambers by the iris (Fig. 3D).

Limbus

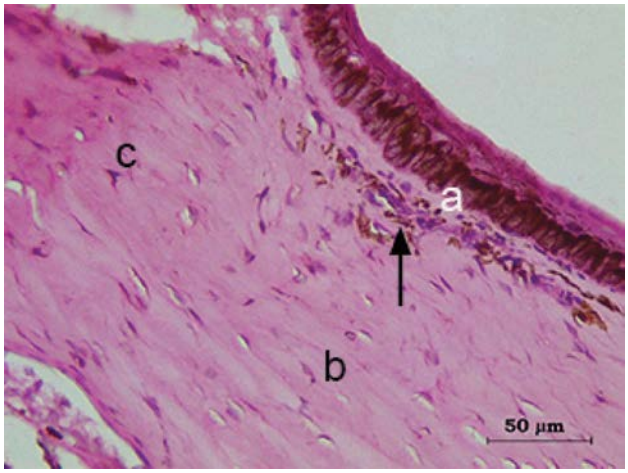

Fig. 4. Photomicrograph of the limbus of tree squirrel. Pigmented cuboidal to columnar basal epithelium: (a) with pigmented stromal cells (arrow) at meeting point of sclera (b); and cornea (c). Haematoxylin-Eosin stain.

The cornea and sclera met at where the sheets of collagen fibres of the two structures combine together. The meeting point was the limbus. The limbus was particularly marked by pigmented cuboidal to columnar epithelia cells at the basal border. Connective tissue cells within this region were pigmented as well. The basal cells of the bulbar conjunctival epithelium continuing from the limbus were more heavily pigmented, more densely populated, smaller and had more irregular arrangement (Fig. 4).

Choroid

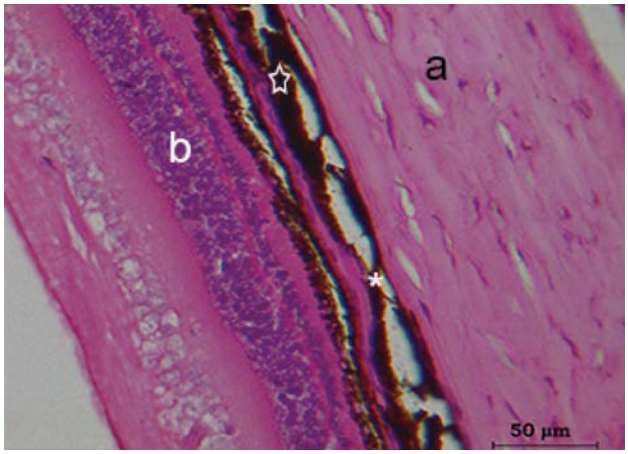

Fig. 5. Photomicrograph of the choroid of tree squirrel.
Melanocyte-rich choroid (star) enmeshed between sclera (a) and photosensitive retina (b) comprises fine network of connective tissue (*) possibly laden with a lot of blood vessel. Hematoxylin-Eosin stain.

The structural component that somewhat sandwiched the photosensitive retina and the sclera was the choroid. It had loose connective tissue that embedded lots of blood vessels and laden with many melanocytes. The choroid vascular bed was linked with sclera via intricate interconnections of suprachoroid connective tissue (Fig. 5).

Ciliary body/Iris

Extension of the choroid anteriorly was the ciliary body comprising smooth muscle fibres in loose connective tissue (Fig. 6A). *Pars ciliaris retinae* was the non-photoreceptor aspect of retina continuing as a bilayer epithelial covering of the ciliary body. Non-pigmented columnar cells formed the outer part of this bilayer while the inner part was formed by pigmented cuboidal cells (Fig. 6A). Folds emerged posteriorly to form the ciliary processes, presenting large surface areas by the tortuous nature (Fig. 6B, C).

The ciliary body was connected to the base of the iris extending between the lens and cornea thus dividing the space into the anterior and posterior chambers (Fig. 6B).

Iris

The connective tissue stroma of the iris was well vascularized with lots of pigmented cells (melanocytes) and sphincter/constrictor muscle fibres. While non-epithelial cells (stromal cells) cover iris anteriorly, the posterior side was composed of two layers of epithelial cells which extended the non-photoreceptor retina otherwise known as the *pars iridica retinae*. Outer aspect of the non-photoreceptor retina was loaded with melanin-pigment copiously but the inner aspect comprised less pigmented contractile myoepithelial cells (dilator muscle) (Fig. 6D).

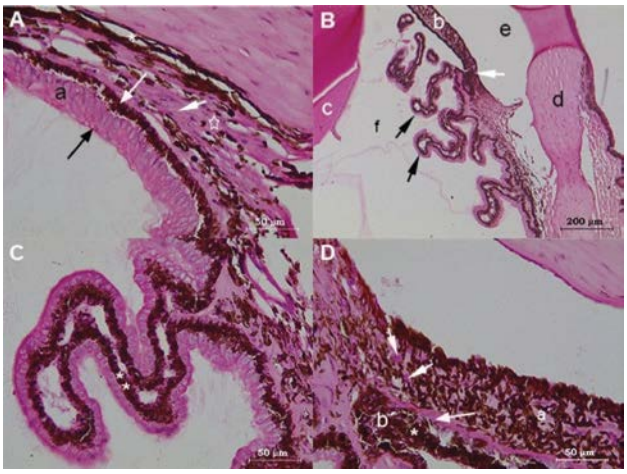

Fig. 6. Photomicrograph of the ciliary body (A-C) and iris (D) of tree squirrel.
Smooth muscle fibres (short-tailed white arrow) in loose connective tissue of ciliary body (star) extending choroid (*) anteriorly and covered by a double layered non-photosensitive retina, Pars ciliaris retinae (a) with pigmented cuboidal inner (long-tailed white arrow) and 2–3 rows of non-pigmented columnar outer cells (black arrow). (B) Folds of non-photosensitive retinae forming tortuous ciliary processes (black arrows) while base (white arrow) of iris (b) is joined with ciliary body. Elongated iris divides space between lens (c) and cornea (d) into anterior (e) and posterior (f) chambers. (C) Ciliary process at higher magnification. Note the non-pigmented superficial but strongly pigmented basal cells (**) of the epithelium. (D) Anteriorly, vascularized stroma (a´) of iris is rich in melanocytes and constrictor muscle fibre (short-tailed arrows) while posteriorly, non-photosensitive retina is continued by the Pars iridica retinae (b´) composed of highly pigmented outer (*) but less pigmented inner myoepithelial cells (long-tailed white arrow).
Hematoxylin-Eosin stain, A-D.

Lens

This epithelial structure was covered entirely by a pale homogenous capsule. The epithelial lining of the lens (lens epithelium) anteriorly was simple cuboidal whereas the structure was devoid of epithelial cells posteriorly (Fig. 7A). The germinal zone near the lens equator comprised freshly laid lens fibres with cells known to have the potential of self-proliferation. More matured fibres became anucleated towards the central part of the lens (Fig. 7B).

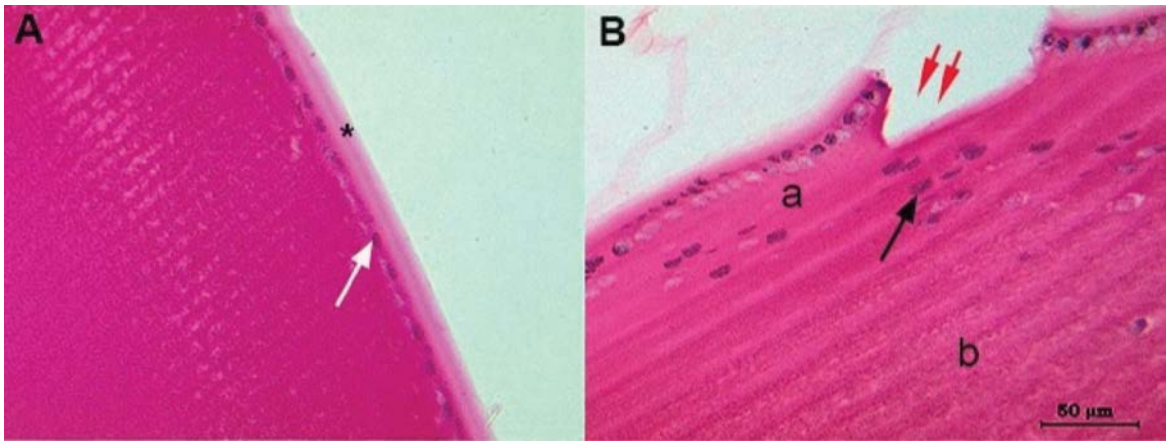

Fig. 7. Photomicrograph of the lens of tree squirrel.
(A) Simple cuboidal epithelium (white arrow) of anterior portion of lens overlayed superficially with homogenous capsule (*), no epithelial cells in the more posterior portion. (B) Proliferative cells (black arrow) of the germinal zone (a). Cells at more central part (b) of lens are anucleated, processing artefacts (double red arrows). Haematoxylin-Eosin stain, A-B.

Retina

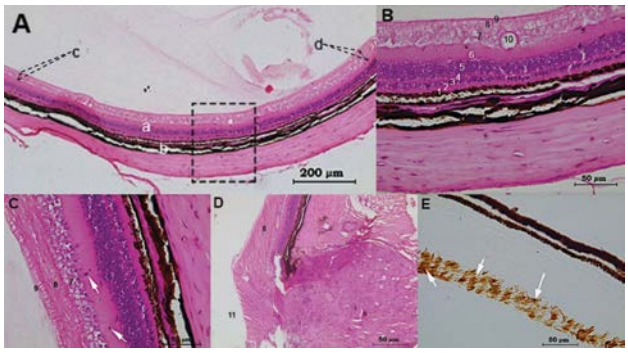

Fig. 8. Retinal cross sections of tree squirrels.
(A) The retina (a) is the photosensitive structure on the inner aspect of choroid (b) organized in multiple layers. The rows of nuclei in the ganglion cell layer and the nerve fibres/limiting membrane increase in thickness (c < d) towards the optic disc. (B) Boxed area in A, the retina multiple layers include, from the outermost, the pigmented epithelium (1), photoreceptor cell layer (rods and cones) (2), outer nuclear layer (3), outer plexiform layer (4), inner nuclear layer (5), inner plexiform layer (6), ganglion cell layer (7), nerve fibre layer (8) and inner limiting membrane (9). While the inner nuclear/plexiform layer is thicker than the outer, the ganglion cells are densely populated with occasional blood vessels (10) traversing the layer. (C) Increased thicknesses of ganglion cell (7), nerve fibre (8) and inner limiting membrane (9) layers of retina towards the optic disc relative to more peripheral aspect (B), displaced retinal ganglion cells (arrows). (D) Nerve fibre layer (8) is thickest at the optic disc (11) region. (E) Dense astrocytic dendritic fibres (short-tailed arrows) of $GFAP^+$ cellular immunoreaction (soma, long-tailed arrow) at the nerve fibre layer. Haematoxylin-Eosin stain, A-D; immunohistochemistry, E.

The retina was the photosensitive structure on the inner aspect of choroid organized in multiple layers corresponding to the typical eye structure of mammals. These layers include, from the outermost, the pigmented cuboidal epithelium, photoreceptor cell layer (outer and inner segments of rods and cones), outer nuclear layer, outer plexiform layer, inner nuclear layer, inner plexiform layer, ganglion cell layer, nerve fibre layer and inner limiting membrane (Fig. 8A-C). While the inner nuclear/plexiform layer is thicker than the outer, a dense ganglion cell layer (GCL) that suggested a higher retina ganglion cell (RGC) density was characterized by occasional relatively large blood vessels traversing the layer and the nerve fibres/limiting membrane increasing in thickness towards the optic disc (Fig 8D). While cells in the ganglion cell layer formed two or more layers, especially at the more central portion, few cells were observed to spill over to the inner plexiform layer (Fig. 8A-C). Astrocytes appeared to wrap thick bundles of their dendrites around the neuronal axons at the nerve fibre layer (Fig. 8E).

Optic nerve

The optic nerve fibre was formed by the convergence of the ganglion cell axonal processes at the optic disc. These axonal processes exited through the *lamina cribosa* of sclera and they appeared to be myelinated at this level seemingly enlarging the axonal diameter (Fig. 9A). Processes of astrocytes forming rich latticework around the head of the optic nerve constituted the glial lamina (Fig. 9B).

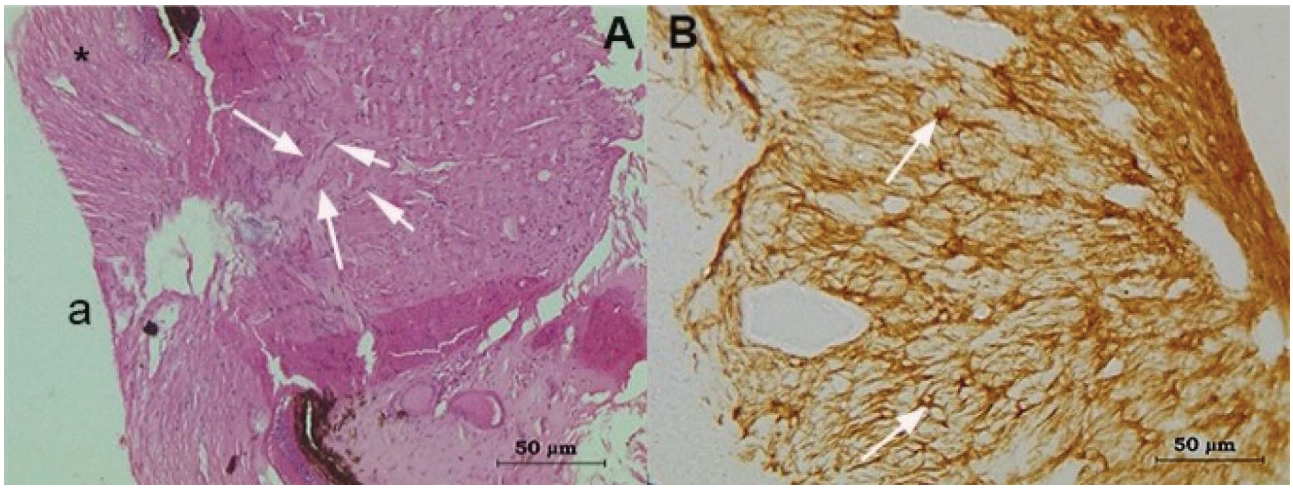

Fig. 9. Photomicrograph of the optic nerve of tree squirrel.
(A) Processes of axons (*) of ganglion cells converging at optic disc (a) forming the optic nerve fibres (long-tailed arrows) piercing through the lamina cribosa of sclera/glial lamina (short-tailed arrows). (B) Latticework of astrocytic processes, glial lamina, of GFAP+ cells (arrows) at the optic nerve. Haematoxylin-Eosin stain, A; immunohistochemistry, B.

Table 1. Corneal, scleral and retinal thicknesses of the Thomas's Rope and Gambian Sun squirrel

Cornea	Mean ± SEM (µm) 422 ± 66.8	Range (µm) 355–489	Percentage contribution to overall thickness (%)
Corneal endothelium	4.44 ± 0.76	3.68–5.2	1
Corneal stroma	351 ± 52.5	299–404	83
Corneal epithelium	63.8 ± 13	50.8–76.8	15
Sclera	134 ± 7.88	126–142	-
Retina	122 ± 2.98	119–125	-
Retinal pigmented epithelium	6.55 ± 0.73	5.83–7.28	5
Photoreceptor cell layer	15.5 ± 0.66	14.8–16.2	13
Outer nuclear layer	5.59 ± 0.29	5.3–5.88	5
Outer plexiform layer	4.9 ± 0.2	4.7–5.1	4
Inner nuclear layer	22.8 ± 1.96	20.9–24.8	19
Inner plexiform layer	23.1 ± 0.25	22.8–23.3	19
Ganglion cell layer	27 ± 4.68	22.3–31.6	22
Nerve fibre layer	12.8 ± 0.78	12–13.5	10
Inner limiting membrane	1.48 ± 0.23	1.25–1.7	1

DISCUSSION

Thomas Rope and Gambian Sun squirrels are diurnal rodents found across West Africa, Nigeria inclusive. These arboreal rodents have some peculiar eye structures bearing some similarities with mammalian visual system and which apparently support their high visual acuity [52, 78].

Cornea/Sclera

Fibres of collagen densely arranged within the cornea and sclera possibly make the eyes pliant and strong enough to withstand pressure changes especially involved in aqueous humour homeostasis that is capable of compromising the eyeball structural makeup [23]. The eyeball is possibly further protected from external insults by the multi-layered (stratified) epithelium of the cornea.

In comparison to the cornea, the sclera is notably more opaque and rigid. It exhibits regional vascularity but lacks epithelial or endothelial surfaces. The sclera is characterized by a moderately rich nerve supply, particularly around episcleral blood vessels, and it lacks lymphatic channels. Scleral fibroblasts demonstrate a complex arrangement within the fibroblast network, often displaying a three-dimensional organization. Additionally, the cellular density of scleral fibroblasts surpasses that of corneal keratocytes, suggesting a more active role in scleral metabolism.

Cornea

Corneal morphology of the tree squirrels investigated in this study has close similarities to those of other domestic mammals [64]. The distinct corneal layers observed in these rodents were: squamous epithelium, collagenous stroma, and endothelium. This particular structural arrangement is known for the majority of vertebrates, human inclusive [6, 17, 21].

The bulk of the corneal thickness (83 %) made up of compact connective tissue constituting the stroma is in line with what is reportedly obtainable in the majority of animals (90 %) [18] even though observed to be higher than that reported for African grasscutter (78 %) [69]. Also, the squirrel cornea overall thickness in the current study (~422 µm) (Table 1) is noticeably thicker relative to grasscutter (~257 µm) [69] and mouse (~80 µm) [76]. It was interesting to note this thickness value the in squirrel is more comparable to that in humans (~550 µm) [29] than in the grasscutter, a rodent of relatively bigger body size. This observation suggests the adaptability of the squirrel cornea to its diurnal lifestyle just like in humans but in contrast to the nocturnal nature of mouse and grasscutter. The tree squirrels understudied in this work could therefore represent a good model for cornea research in humans [7, 63, 73].

In spite of the strongly PAS-stained corneal epithelial basement membrane, Bowman's membrane appears not demonstrable in the squirrel species examined in this study. While early reports have indicated that rodent species lack Bowman's membrane [42, 86], its presence in rats and mice has been documented by an electron microscopic investigation [36]. Peter-Ajuzie, Nwaogu and Igwe buike [69] also reported the lack of Bowman's membrane in other rodents like grasscutter while in some domestic animals, PAS reactivity indicated that this membrane is absent [64]. However, Peter-Ajuzie et al. [68] showed that the African straw-coloured fruit bat possess a thin layer of Bowman's membrane in its cornea. The exact functionality of the Bowman's membrane is yet to be proven and although present in avian and primate's eyes [58], other domestic mammals having this membrane has also not been clarified yet [64].

Glycogen, a reservoir for energy supply, as well as glycoproteins have been demonstrated in cornea of cattle [87], rabbit [53] and humans [32]. The strong PAS positivity of corneal epithelial layer noted in this study indicates that this superficial layer has a possible high glycogen content which could further translates to elevated aerobic glycolysis with accentuated metabolic activity [1]. This biological requirement is essential to achieve accommodation of objects in the eyes of this rodent species necessary for survival in their arboreal habitat. Similar observations have been documented in certain avians [3]. This nonetheless calls for additional investigation using more specific staining techniques, immunohistochemistry for instance, to elucidate further on the structural compositions of the African tree squirrel cornea [64].

Ciliary body/Iris

The current work describes a fairly developed ciliary body unlike those in grasscutter [69] as well as rabbit and some rodents [22, 89]. High visual acuity of squirrels also entails sharp lenticular accommodation required for their diurnal behavioural nature. The structural arrangement of the non-photosensitive part of retina (*Pars ciliaris retinae*) is similar to those described in mammals generally. However, Peter-Ajuzie et al. [69] reported melanin content of the superficial layer of the *Pars ciliaris retinae* of grasscutter which possibly represents a changeover of the ciliary body histoarchitecture to that of iris.

The aqueous humour is presumably generated from the ciliary epithelial cells. Therefore, the broad surface area provided by the tortuous ciliary processes noticeable in the tree squirrel eyes likely serves the function of generating sufficient humour. This anatomical feature has been detailed also in a diurnal desert rodent [74] and in some experimental rodent species as well [14].

Previous investigation on mammals that are diurnal in nature and arrhythmic have documented copious melanin pigmentation with high vascularity and well-formed sphincter muscle fibres characterizing the ciliary body/iris [50, 74] which are in conformity to those reported in this study. The high iridal melanin content observed in the tree squirrel species studied here could possibly serve to limit light rays entry only via the pupil [55] while pupillary contraction has a protective effect on the retina in situation where light intensity is increased instantly [86].

In addition, regarding the strong pigmentation of the profusely vascular choroid including the retinal pigmented epithelium, we speculate that the tree squirrel eye has higher capacity to endure extreme solar emissions [46] in comparison to their counterpart nocturnal rodents.

Retina

The retina of the tree squirrels examined in the current study has a mammal's typical structural organization.

The mean thickness of the retina (~122 μm) (Table 1) is thinner in comparison to some murines: rat (~220 μm), possum (~170 μm) and guinea pig (~140 μm) [11]. This apparently reflects the nocturnal lifestyle adaptation of these other rodent species. In other for those murines to be more receptive to light, they possess more populations of rod photoreceptors, long and slender, contributing to the relatively thicker retinas [50] when compared to the diurnal squirrel species. This finding concurs with a previous report concerning diurnal desert rodents [74].

Pigmented epithelium occurring in the entire structure of squirrel as also reported for grasscutter [69] unlike other mammals is indicative of the absence of tapetum lucidum. This eye anatomic component being reflective in nature facilitates sight capacity in dim light circumstances particularly in crepuscular, cathemeral and nocturnal subjects [69]. Squirrels as diurnal rodents do not need this structure as majority of rodents reportedly lack tapetum lucidum [71]. Thus in conformity with their diurnal lifestyle, the highly pigmented epithelium in the squirrel retina stops too much ultraviolet rays reaching the transparent scleral tunic as it absorbs light, thus minimizing scatter inside the eye structure [47, 86].

High visual acuity of squirrels is further supported by the presence of elevated retinal ganglion cell density which compares to that in human and other phototopic subjects [83]. This observed feature contrasted the report on grasscutter [69] with scanty ganglion cells in line with the nocturnal characteristics and inferior visual acuity of this rodent species [35].

Relatively large blood vessels occasionally feature in the ganglion cell layer possibly to facilitate supply of oxygen and nutrients to meet the metabolic demands of the densely populated retinal final-output neuronal cells which project to the visual regions of the brain such as the lateral geniculate nucleus and superior colliculi. Projections from these regions then ultimately reach the primary visual cortex.

The dense cellular population and multiple layering observed at the retinal ganglion cell layer in these tree-harbouring rodent species suggest cone-dominated photoreceptor neurons in the retina [48] concurring with those reported in the ground squirrels [90]. These findings further highlight the closer semblance of the retina of these diurnal animals to those of primates/humans when compared with other rodents that are nocturnal [33, 60, 61, 75].

Neuronal cells, RGCs in particular, within retinal layer of ganglion cells project their axonal processes to link visual brain regions with the eye via the optic nerve fibres [70]. The current work demonstrated astrocytic dendritic bundles densely wrapping the neuronal axons as shown by the GFAP immunohistochemistry in the retina and optic nerve. These findings have been similarly documented in a previous study on thirteen lined ground squirrel [90]. The rich latticework of astrocytic processes of the well-developed glial lamina noted in these tree squirrel species is close to what is found in the arrangement of human optic nerve/*lamina cribosa* ultimately reflecting the rodents' diurnal nature [37, 43].

Such structural interconnection observed to be present in the retina of primates modulates ganglion cell axonal injury [34] and by extension on pathology of optic nerve as well [37] particularly via astrocytic response [57]. Moreover, optic nerve impairment resulting in alterations in axons of retinal ganglion cells facilitates the neurons' progressive death [33, 56, 59, 60, 62, 67, 85,] and the impairment is a potential cause of irreparable blindness [13]. The findings thus documented in this study further show that squirrels are better models for human eye research than rats and mice [7, 63, 73, 84, 90].

The few population of cells noted outside the ganglion cell layer of the animals investigated in the current work, towards the inner plexiform layer, are otherwise called displaced retinal ganglion cells [24, 25, 26, 61] and could possibly represent amacrine cells [90]. These observed nuclei, within the inner plexiform layer, representing endothelial cells are not ruled out though. Further investigations such as cell quantifications [44, 51] and immunohistochemical characterization [8, 9, 10, 80] are thus needed to understudy these densely populated ganglion cells including astrocytic population of the optic nerve of the African tree squirrels to establish comparative analysis, with ground squirrels [90] for instance.

CONCLUSIONS

Conclusively, Thomas's rope and Gambian Sun squirrels possess arboreal-habitat-fitted visual structural make-

up supported mainly by elaborate ganglion cells in the retina and much thickness of the corneal stroma. These species' apparent lack of *tapetum lucidum* has further given credence to their diurnal nature while the retinal histo-morphometric data presented is also useful for prospective investigations of rodent visual system. Additionally, findings documented in this study share some similarities with the human visual system suggesting that these tree squirrels are great models to understudy retinal/ocular system in humans.

ACKNOWLEDGEMENT

We are grateful to Humboldt Research Hub for Zoonotic Arbovirus Disease (HRH-ZAD), University of Ibadan, Ibadan, Nigeria, for the supply of experimental animals and resource materials.

The authors declare that this work was in part funded by Humboldt Research Hub for Zoonotic Arboviral Diseases (HRH-ZAD) grant to J.O.O.

Competing Interests

The authors have no relevant financial or non-financial interests to disclose.

Data availability statement

All data related to this manuscript will be made available by the corresponding author upon request.

REFERENCES

1. **Abdelftah, Z., Gaber, A. R., Abo-Eleneen, R. E., EL-Bakry, A. M., 2021:** Microstructure characteristics of cornea of some birds: A comparative study. *Beni-Suef Univ. J. Basic. Appl. Sci*., 10, 1, 66. Available at https://bjbas.springeropen.com/articles/10.1186/s43088-021-00155-2.
2. **Agrawal, R. N, He, S., Spee, C., Cui, J. Z., Ryan, S. J., Hinton, D. R., 2007:** In vivo models of proliferative vitreoretinopathy. *Nat. Protoc*., 2, 1, 67–77. Available at http://www.nature.com/articles/nprot.2007.4.
3. **Albuquerque, L., Pigatto, J. A. T., Freitas, L. V. da RP., 2015:** Analysis of the corneal endothelium in eyes of chickens using contact specular microscopy. *Semin Ciências Agrárias*, 36, 6, Supl. 2, 4199. Available at http://www.uel.br/revistas/uel/index.php/semagrarias/article/view/19497.
4. **Bamidele, A. O., Akinpelu, A. I., 2020:** Comparison of cranial and body morphology of tree squirrels (*Helioscurius rufobranchium*) in selected locations of rainforest in Nigeria. *Zool*., 17, 47–53. Available at https://www.ajol.info/index.php/tzool/article/view/193735.
5. **Bancroft, J. D., Layton, C., 2013:** The hematoxylins and eosin. In **Suvarna, S. K., Layton, C., Bancroft, J. D.:** *Bancroft's Theory and Practice of Histological Techniques*. 7th edn., Churchill Livingstone, UK, 173–86. Available at https://linkinghub.elsevier.com/retrieve/pii/B978070204226300010X.
6. **Beuerman, R. W., Pedroza, L., 1996:** Ultrastructure of the human cornea. *Microsc. Res. Tech*., 33, 4, 320–335. DOI: 10.1002/(SICI)1097-0029(19960301)33:4%3C320::AID-JEMT3%3E3.0.CO;2-T.
7. **Brunette, I., Rosolen, S. G., Carrier, M., Abderrahman, M., Nada, O., Germain, L., et al., 2011:** Comparison of the pig and feline models for full thickness corneal transplantation. *Vet. Ophthalmol*., 14, 6, 365–377. DOI: 10.1111/j.1463-5224.2011.00886.x.
8. **Butt, A. M., Colquhoun, K., Tutton, M., Berry, M., 1994:** Three-dimensional morphology of astrocytes and oligodendrocytes in the intact mouse optic nerve. *J. Neurocytol*., 23, 8, 469–485. Available at http://link.springer.com/10.1007/BF01184071.
9. **Butt, A. M., Ransom, B. R., 1989:** Visualization of oligodendrocytes and astrocytes in the intact rat optic nerve by intracellular injection of lucifer yellow and horseradish peroxidase. *Glia*, 2, 6, 470–475. DOI: 10.1002/glia.440020609.
10. **Butt, A. M., Ransom, B. R., 1993:** Morphology of astrocytes and oligodendrocytes during development in the intact rat optic nerve. *J. Comp. Neurol*., 338, 1, 141–158. DOI: 10.1002/cne.903380110.
11. **Buttery, R. G., Hinrichsen, C. F. L., Weller, W. L., Haight, J. R., 1991:** How thick should a retina be? A comparative study of mammalian species with and without intraretinal vasculature. *Vision Res*, 31, 2, 169–187. Available at https://linkinghub.elsevier.com/retrieve/pii/004269899190110Q.
12. **Campi, K. L., Krubitzer, L., 2010:** Comparative studies of diurnal and nocturnal rodents: Differences in lifestyle result in alterations in cortical field size and number. *J. Comp. Neurol.*, 518, 22, 4491–4512. DOI: 10.1002/cne.22466.
13. **Case, L. C., Tessier-Lavigne, M., 2005:** Regeneration of the adult central nervous system. *Curr. Biol*., 15, 18, R749–753.

Available at https://linkinghub.elsevier.com/retrieve/pii/S0960982205010304.

14. **Cech, S., 2004:** An attempt to describe the ultrastructure and ultrahistochemistry of ciliary processes in mammals. *Biomed. Pap. Med. Fac. Univ. Palacky Olomouc Czech Repub*., 148, 2, 201–202. DOI: 10.5507/bp.2004.038.html.
15. **Cernuda-Cernuda, R., García-Fernández, J. M., Gordijn, M. C. M., Bovee-Geurts, P. H. M., DeGrip, W. J., 2003:** The eye of the African mole-rat *Cryptomys anselli*: To see or not to see? *Eur. J. Neurosci*., 17, 4, 709–720. DOI: 10.1046/j.1460-9568.2003.02485.x.
16. **Chakravarthy, A. K., Thyagaraj, N. E., 2012:** The palm squirrel in coconut plantations: ecosystem services by therophily. *Mammalia*, 76, 2. DOI: 10.1515/mammalia-2011-0073/html.
17. **Chakravarti, S., 2001:** The cornea through the eyes of knockout mice. *Exp. Eye Res*., 73, 4, 411–9. Available at https://linkinghub.elsevier.com/retrieve/pii/S0014483501910553.
18. **Cholkar, K., Dasari., S. R., Pal, D., Mitra, A. K., 2013:** Eye: Anatomy, physiology and barriers to drug delivery. In *Ocular Transporters and Receptors*. 1–36. Available at https://linkinghub.elsevier.com/retrieve/pii/B9781907568862500010
19. **Coker, O. M., Jubril, A. J., Isong, O. M., Omonona, A. O., 2020:** Internal and external morphometry of Thomas's rope squirrel (*Funisciurus anerythrus*) and Gambian sun squirrel (*Heliosciurus gambianus*) in Ibadan, Nigeria. *Anim. Res. Int*., 17, 2, 3747–3760. Available at https://www.ajol.info/index.php/ari/article/view/199339.
20. **Coker, O. M., Osaiyuwu, O. H., Isong, O. M., 2020:** Genetic variations in Thomas's Rope squirrel (*Funisciurus anerythrus*) and Gambian Sun squirrel (*Heliosciurus gambianus*) Ibadan, Nigeria, using allozyme markers. *Genet. Biodivers. J*., 5, 1, 4–11. Available at https://journals.univ-tlemcen.dz/GABJ/index.php/GABJ/article/view/158.
21. **Collin, S. P., Collin, H. B., 1998:** A comparative study of the corneal endothelium in vertebrates. *Clin. Exp. Optom*., 81, 6, 245–254. DOI: 10.1111/j.1444-0938.1998.tb06744.x.
22. **Davis, F. A., 1929:** The anatomy and histology of the eye and orbit of the rabbit. *Trans. Am. Ophthalmol. Soc*., 27, 400.2–441. Available at http://www.ncbi.nlm.nih.gov/pubmed/16692841.
23. **Davis, K., Carter, R., Tully, T., Negulescu, I., Storey, E., 2015:** Comparative evaluation of aqueous humour viscosity. *Vet. Ophthalmol*., 18, 1, 50–8. DOI: 10.1111/vop.12145.
24. **Dogiel, A. S. 1895:** Die Retina der Vögel. *Arch. für Mikroskopische Anat*., 44, 1, 622–648. Available at http://link.springer.com/10.1007/BF02934032.
25. **Doi, M., Imatani, H., Sasoh, M., Uji, Y., Yamamura, H., 1994:** Displaced retinal ganglion cells in the Chinese hamster. *Jpn. J. Ophthalmol*., 38, 2, 139–143. Available at http://www.ncbi.nlm.nih.gov/pubmed/7967204.
26. **Dräger, U. C., Olsen, J. F., 1980:** Origins of crossed and uncrossed retinal projections in pigmented and albino mice. *J. Comp. Neurol*., 191, 3, 383–412. DOI: 10.1002/cne.901910306.
27. **Duke-Elder, S., 1958:** The eye in evolution. In *System of Ophthalmology,* 19 Volume Set. London, Henry Kimpton, 14392 pp.
28. **Duncan, R. D., Jenkins, S. H., 1998:** Use of visual cues in foraging by a diurnal herbivore, Belding's ground squirrel. *Can. J. Zool*., 76, 9, 1766–1770. DOI: 10.1139/z98-119.
29. **Fatt, I., Weissman, B. A., 2013:** *Physiology of the Eye: An Introduction to the Vegetative Functions*. Elsevier Science, 517 pp. Available at https://www.everand.com/book/282595670/Physiology-of-the-Eye-An-Introduction-to-the-Vegetative-Functions.
30. **Fitch, H. S., 1948:** Ecology of the California ground squirrel on grazing lands. *Am. Midl. Nat*., 39, 3, 513. Available at https://www.jstor.org/stable/2421524?origin=crossref.
31. **Fitzgibbon, C. D., Mogaka, H., Fanshawe, J. H., 1995:** Subsistence hunting in Arabuko-Sokoke forest, Kenya, and its effects on mammal populations. *Conserv. Biol*., 9, 5, 1116–1126. DOI: 10.1046/j.1523-1739.1995.9051085.x-i1.
32. **Gabriel, L. A. R., Wang, L. W., Bader, H., Ho, J. C., Majors, A. K., Hollyfield, J. G., et al., 2012:** ADAMTSL4, a secreted glycoprotein widely distributed in the eye, binds fibrillin-1 microfibrils and accelerates microfibril biogenesis. *Invest. Ophthalmol. Vis. Sci*., 53, 1, 461–469. Available at http://www.ncbi.nlm.nih.gov/pubmed/21989719.
33. **Galindo-Romero, C., Avilés-Trigueros, M., Jiménez-López, M., Valiente-Soriano, F. J., Salinas-Navarro, M., Nadal-Nicolás, F., et al., 2011:** Axotomy-induced retinal ganglion cell death in adult mice: quantitative and topographic time course analyses. *Exp. Eye Res*., 92, 5, 377–387. Available at https://linkinghub.elsevier.com/retrieve/pii/S001448351100042X.
34. **Guttenplan, K. A., Stafford, B. K., El-Danaf, R. N., Adler, D. I., Münch, A. E., Weigel, M. K., et al., 2020:** Neurotoxic reactive astrocytes drive neuronal death after retinal injury. *Cell. Rep*., 31, 12, 107776. Available at https://linkinghub.elsevier.com/retrieve/pii/S2211124720307567.
35. **Hall, M. I., 2008:** Comparative analysis of the size and shape of the lizard eye. *Zoology* (Jena), 111, 1, 62–75.

Available at https://linkinghub.elsevier.com/retrieve/pii/S0944200607000785.

36. **Hayashi, S., Osawa, T., Tohyama, K., 2002:** Comparative observations on corneas, with special reference to Bowman's layer and Descemet's membrane in mammals and amphibians. *J. Morphol*., 254, 3, 247–258. DOI: /10.1002/jmor.10030.
37. **Howell, G. R., Libby, R. T., Jakobs, T. C., Smith, R. S., Phalan, F. C., Barter, J. W., et al., 2007:** Axons of retinal ganglion cells are insulted in the optic nerve early in DBA/2J glaucoma. *J. Cell. Biol*., 179, 7, 1523–1537. Available at http://www.ncbi.nlm.nih.gov/pubmed/18158332.
38. **Ikpegbu, E., Nlebedum, U., Ibe, C., 2014:** The kidney and adrenal gland of the African palm squirrel *Epixerus ebii*: A microanatomical observation. *Rev. Fac. Ciencias. Vet*., 55, 2, 60–67. Available at https://www.redalyc.org/pdf/3731/373139085001.pdf.
39. **Ikyaagba, E. T., Alarape, A. A., Omifolaji, J. K., Uloko, I. J., Jimoh, O. S., 2020:** Mammal richness and diversity in tropical ecosystem: The role of protected area in conserving vertebrate fauna, Oban Hill's region. *J. Agric. Sustain*., 13, 1–20. Available at https://infinitypress.info/index.php/jas/article/view/1975.
40. **Jackson, P., Blythe, D., 2013:** Immunohistochemical techniques. In **Suvarna, S. K., Layton, C., Bancroft, J. D.:** *Bancroft's Theory and Practice of Histological Techniques.* 7th edn., Elsevier, 381–426. Available at https://linkinghub.elsevier.com/retrieve/pii/B9780702042263000184.
41. **Jacobs, G. H., Tootell, R. B. H., Fisher, S. K., Anderson, D. H., 1980:** Rod photoreceptors and scotopic vision in ground squirrels. *J. Comp. Neurol*., 189, 1, 113–125. DOI: 10.1002/cne.901890107.
42. **Jakus, M. A., 1954:** Studies on the cornea. I. The fine structure of the rat cornea. *Am. J. Ophthalmol.,* 38, 1, 2, 40–53. Available at http://www.ncbi.nlm.nih.gov/pubmed/13180617.
43. **Jeffery, G., Evans, A., Albon, J., Duance, V., Neal, J., Dawidek, G., 1995:** The human optic nerve: Fascicular organisation and connective tissue types along the extra-fascicular matrix. *Anat. Embryol.* (Berl)., 191, 6, 491–502. Available at http://link.springer.com/10.1007/BF00186739.
44. **Johnson, P. T., Geller, S. F., Reese, B. E., 1998:** Distribution, size and number of axons in the optic pathway of ground squirrels. *Exp. Brain Res*., 118, 1, 93–104. Available at http://link.springer.com/10.1007/s002210050258.
45. **Kingdon, J., 1997:** *The Kingdon Field Guide to African Mammals*. Academic Press, San Diego, California. Available at http://www.rhinoresourcecenter.com/pdf_files/130/1303945154.pdf.
46. **Koskela, T. K., Reiss, G. R., Brubaker, R. F., Ellefson, R. D., 1989:** Is the high concentration of ascorbic acid in the eye an adaptation to intense solar irradiation? *Invest. Ophthalm. Vis. Sci*., 30, 10, 2265–2267. Available at http://www.ncbi.nlm.nih.gov/pubmed/2793364.
47. **Kronfeld-Schor, N., Dayan, T., Jones, M. E., Kremer, I., Mandelik, Y., Wollberg, M., et al., 2001:** Retinal structure and foraging microhabitat use of the golden spiny mouse (*Acomys russatus*). *J. Mammal*., 82, 4, 1016–1025. Available at https://academic.oup.com/jmammal/article/82/4/1016-1025/2372725.
48. **Kryger, Z., Galli-Resta, L., Jacobs, G. H., Reese, B. E., 1998:** The topography of rod and cone photoreceptors in the retina of the ground squirrel. *Vis. Neurosci*., 15, 4, 685–691. Available at https://www.cambridge.org/core/product/identifier/S0952523898154081/type/journal_article.
49. **Layton, C., Bancroft, J. D., 2013:** Carbohydrates. In: **Suvarna, S. K., Layton, C., Bancroft, J. D.:** *Bancroft's Theory and Practice of Histological Techniques* (Internet). 7th edn., Churchill Livingstone, UK, 215–238. Available at https://linkinghub.elsevier.com/retrieve/pii/B9780702042263000123.
50. **Lluch, S., Ventura, J., López-Fuster, M. J., 2008:** Eye morphology in some wild rodents. *Anat. Histol. Embryol*., 37, 1, 41–51. DOI: 10.1111/j.1439-0264.2007.00796.x.
51. **Long, K. O., Fisher, S. K., 1983:** The distributions of photoreceptors and ganglion cells in the California ground squirrel, *Spermophilus beecheyi*. *J. Comp. Neurol*., 221, 3, 329–340. DOI: 10.1002/cne.902210308.
52. **Lurz, P., 2011:** Squirrels and relatives II: Ground squirrels. In *Grzimek's Animal Life Encyclopedia: Mammals*, 16, 143–161. Available at https://brookslibraryvt.org/wp-content/uploads/2021/02/Squirrels_and_Relatives_II_Gro.pdf.
53. **Malinin, G. I., Bernstein, H., 1979:** Histochemical demonstration of glycogen in corneal endothelium. *Exp. Eye Res*., 28, 4, 381–385. Available at https://linkinghub.elsevier.com/retrieve/pii/0014483579901131.
54. **McFarland, W. N., 1991:** The visual world of coral reef fishes. In *The Ecology of Fishes on Coral Reefs*. Academic Press, San Diego, California, 16–38. Available at https://www.vliz.be/en/imis?module=ref&refid=9173.
55. **Mescher, A. L., 2016:** *Junqueira's Basic Histology: A Color Atlas and Text*. 14th edn., Basic histology: A colour atlas and text. McGraw-Hill Education, 573 pp. Available at https://www.academia.edu/37006818/Junqueiras_Basic_Histology_Text_and_Atlas_14th_Edition.

56. **Misantone, L. J., Gershenbaum, M., Murray, M., 1984:** Viability of retinal ganglion cells after optic nerve crush in adult rats. *J. Neurocytol*., 13, 3, 449–465. Available at http://link.springer.com/10.1007/BF01148334.
57. **Morgan, W. H., Yu, D. Y., Alder, V. A., Cringle, S. J., Cooper, R. L., House, P. H., et al., 1998:** The correlation between cerebrospinal fluid pressure and retrolaminar tissue pressure. *Invest, Ophthalmol. Vis. Sci*., 39, 8, 1419–1428. Available at http://www.ncbi.nlm.nih.gov/pubmed/9660490.
58. **Müller, L. J., Pels, L., Vrensen, G. F., 1995:** Novel aspects of the ultrastructural organization of human corneal keratocytes. *Invest. Ophthalmol. Vis. Sci*., 36, 13, 2557–2567. Available at http://www.ncbi.nlm.nih.gov/pubmed/7499078.
59. **Nadal-Nicolás, F. M., Jiménez-López, M., Salinas-Navarro, M., Sobrado-Calvo, P., Vidal-Sanz, M., Agudo-Barriuso, M., 2017:** Microglial dynamics after axotomy-induced retinal ganglion cell death. *J. Neuroinflam.*, 14, 1, 218. Available at https://jneuroinflammation.biomedcentral.com/articles/10.1186/s12974-017-0982-7.
60. **Nadal-Nicolás, F. M., Jiménez-López, M., Sobrado-Calvo, P., Nieto-López, L., Cánovas-Martínez, I., Salinas-Navarro, M., et al., 2009:** Brn3a as a marker of retinal ganglion cells: qualitative and quantitative time course studies in naive and optic nerve-injured retinas. *Invest. Ophthalmol. Vis. Sci*., 50, 8, 3860–3868. Available at http://iovs.arvojournals.org/article.aspx?doi=10.1167/iovs.08-3267.
61. **Nadal-Nicolas, F. M., Salinas-Navarro, M., Jiménez-López, M., Sobrado-Calvo, P., Villegas-Pérez, M. P., Vidal-Sanz, M., et al., 2014:** Displaced retinal ganglion cells in albino and pigmented rats. *Front. Neuroanat*., 8, 99. Available at http://www.ncbi.nlm.nih.gov/pubmed/25339868.
62. **Nadal-Nicolás, F. M., Sobrado-Calvo, P., Jiménez-López, M., Vidal-Sanz, M., Agudo-Barriuso, M., 2015:** Long-term effect of optic nerve axotomy on the retinal ganglion cell layer. *Invest. Ophthalmol. Vis. Sci*., 56, 10, 6095–6112. Available at http://iovs.arvojournals.org/article.aspx?doi=10.1167/iovs.15-17195.
63. **Nadal-Nicolás, F., Miyagishima, K., Li, W., 2022:** In search for the "idyllic" animal model to evaluate ocular pathologies and translate new therapies to improve human health. *Neural Regen. Res*., 17, 12, 2697. Available at http://www.ncbi.nlm.nih.gov/pubmed/35662215.
64. **Nautscher, N., Bauer, A., Steffl, M., Amselgruber, W. M., 2016:** Comparative morphological evaluation of domestic animal cornea. *Vet. Ophthalmol*., 19, 4, 297–304. DOI: 10.1111/vop.12298.
65. **Omifolaji, J. K., Teresa, I. E., Alarape, A. A., Ojo, V. A., Modu, M., Lateef, L. F., et al., 2020:** Estimates of Demidoff's galago (*Galagoides demidovii*) density and abundance in a changing landscape in the Oban hills, Nigeria. Hystrix, *Ital. J. Mammal*., 2, 31, 117–122. Available at http://www.italian-journal-of-mammalogy.it/Estimates-of-Demidoff-s-galago-Galagoides-demidovii-density-and-abundance-in-a-changing,128298,0,2.html#.
66. **Omonona, A., Ademola, I., Odeniran, P., Jubril, A., Asenowo, O., Olagbenro, O., 2020:** Parasitic burden of African squirrels captured in a Nigerian University community. *Niger. J. Parasitol*., 41, 2. Available at https://www.ajol.info/index.php/njpar/article/view/200107.
67. **Parrilla-Reverter, G., Agudo, M., Nadal-Nicolás, F., Alarcón-Martínez, L., Jiménez-López, M., Salinas-Navarro, M., et al., 2009:** Time-course of the retinal nerve fibre layer degeneration after complete intra-orbital optic nerve transection or crush: A comparative study. *Vision Res*., 49, 23, 2808–2825. Available at https://linkinghub.elsevier.com/retrieve/pii/S0042698909003794.
68. **Peter-Ajuzie, I. K., Nwaogu, I. C., Majesty-Alukagberie, L. O., Ajaebili, A. C., Farrag, F. A., Kassab, M. A., Abumandour, M., 2022:** Ocular morphology of the fruit bat, *Eidolon helvum*, and the optical role of the choroidal papillae in the megachiropteran eye: A novel insight. *Folia Morphologica*, 81, 3, 715–722. DOI: 10.5603/FM.a2021.0072.
69. **Peter-Ajuzie, I. K., Nwaogu, I. C., Igwebuike, U. M., 2019:** Anatomical assessment of the eye of the African grasscutter (*Thryonomys swinderianus*). *J. Appl. Life Sci. Int*., 1–8. Available at https://journaljalsi.com/index.php/JALSI/article/view/365.
70. **Ramón y Cajal, S., 1972:** *The Structure of the Retina*. Thorpe, S., Glickstein, M., translators. Thomas, Springfield, Illinois, 196 pp.
71. **Rodriguez-Ramos, Fernandez J., Dubielzig, R. R., 2013:** Ocular comparative anatomy of the family Rodentia. *Vet. Ophthalmol.*, 16 Suppl. 1, 94–99. Available at http://www.ncbi.nlm.nih.gov/pubmed/23734597.
72. **Rosevear, D. R., 1969:** *The Rodents of West Africa.* London: British Museum (Natural History), 604 pp. Available at https://books.google.com.ng/books/about/The_Rodents_of_West_Africa.html?id=wUEgSgAACAAJ&redir_esc=y.
73. **Ruiz-Ederra, J., García, M., Hernández, M., Urcola, H., Hernández-Barbáchano, E., Araiz, J., et al., 2005:** The pig eye as a novel model of glaucoma. *Exp. Eye Res*., 81, 5, 561–569. Available at http://www.ncbi.nlm.nih.gov/pubmed/15949799.

74. Saadi-Brenkia, O., Hanniche, N., Lounis, S., 2018: Microscopic anatomy of ocular globe in diurnal desert rodent *Psammomys obesus* (Cretzschmar, 1828). *J. Basic Appl. Zool*., 79, 1, 43. Available at https://basicandappliedzoology.springeropen.com/articles/10.1186/s41936-018-0056-0.

75. Sánchez-Migallón, M. C., Valiente-Soriano, F. J., Nadal-Nicolás, F. M., Vidal-Sanz, M., Agudo-Barriuso, M., 2016: Apoptotic retinal ganglion cell death after optic nerve transection or crush in mice: Delayed RGC loss with BDNF or a caspase 3 inhibitor. *Invest. Ophthalmol. Vis. Sci*., 57, 1, 81–93. Available at http://iovs.arvojournals.org/article.aspx?doi=10.1167/iovs.15-17841.

76. Scott, J. E., Bosworth, T.R., 1990: A comparative biochemical and ultrastructural study of proteoglycan-collagen interactions in corneal stroma. Functional and metabolic implications. *Biochem. J*., 270, 2, 491–497. Available at https://portlandpress.com/biochemj/article/270/2/491/26625/A-comparative-biochemical-and-ultrastructural.

77. Seebeck, J. H., 1989: Scuiridae. In **Walton, D., Richardson, B.:** *Mammalia, Fauna of Australia Series*. Canberra, Australia: Australian Government Publishing Service; 1–13. Available at https://web.archive.org/web/20150117031835/http://www.scarysquirrel.org/vacation/australia/fauna.pdf.

78. Shorten, M., 1954: *Squirrels.* Collins, London, 212 pp.

79. Sondereker, K. B., Stabio, M. E., Jamil, J. R., Tarchick, M. J., Renna, J. M., 2018: Where you cut matters: A dissection and analysis guide for the spatial orientation of the mouse retina from ocular landmarks. *J. Vis. Exp*., 138. Available at https://www.jove.com/t/57861/where-you-cut-matters-dissection-analysis-guide-for-spatial.

80. Sun, D., Lye-Barthel, M., Masland, R. H., Jakobs, T. C., 2009: The morphology and spatial arrangement of astrocytes in the optic nerve head of the mouse. *J. Comp. Neurol*., 516, 1, 1–19. DOI: 10.1002/cne.22058.

81. Szél, A., Röhlich, P., 1988: Four photoreceptor types in the ground squirrel retina as evidenced by immunocytochemistry. *Vision Res*., 28, 12, 1297–1302. Available at https://linkinghub.elsevier.com/retrieve/pii/0042698988900600.

82. Thorington, R. W., Thorington, J. R. W., Ferrell, K. E., 2007: Squirrels: The animal answer guide. *J. Mammal*., 88, 3, 824–824. DOI: 10.1644/06-MAMM-R-397R.1.

83. Vajzovic, L., Hendrickson, A. E., O'Connell, R. V., Clark, L. A., Tran-Viet, D., Possin, D., et al., 2012: Maturation of the human fovea: correlation of spectral-domain optical coherence tomography findings with histology. *Am. J. Ophthalmol*., 154, 5, 779–789.e2. Available at http://www.ncbi.nlm.nih.gov/pubmed/22898189.

84. Van Hooser, S. D., Nelson, S. B., 2006: The squirrel as a rodent model of the human visual system. *Vis. Neurosci*., 23, 5, 765–778. Available at https://www.cambridge.org/core/product/identifier/S0952523806230098/type/journal_article

85. Villegas-Pérez, M. P., Vidal-Sanz, M., Rasminsky, M., Bray, G. M., Aguayo, A. J., 1993: Rapid and protracted phases of retinal ganglion cell loss follow axotomy in the optic nerve of adult rats. *J. Neurobiol*., 24, 1, 23–36. DOI: 10.1002/neu.480240103.

86. Walls, G. L., 1963: *The Vertebrate Eye and its Adaptative Radiation.* Hafner Publishing Co., New York, London, 785 pp. Available at https://ia802605.us.archive.org/35/items/vertebrateeyeits00wall/vertebrateeyeits00wall.pdf.

87. Wasilewa, P., Hockwin, O., Korte, I., 1976: Glycogen concentration changes in retina, vitreous body and other eye tissues caused by disturbances of blood circulation. *Albrecht Von Graefes Arch. Klin. Exp. Ophthalmol*, 199, 2, 115–120. Available at http://www.ncbi.nlm.nih.gov/pubmed/1083690.

88. West, R. W., Dowling, J. E., 1975: Anatomical evidence for cone and rod-like receptors in the gray squirrel, ground squirrel, and prairie dog retinas. *J. Comp. Neurol*., 159, 4, 439–460. DOI: 10.1002/cne.901590402.

89. Woolf, D., 1956: A comparative cytological study of the ciliary muscle. *Anat. Rec*., 124, 2, 145–163. Available at http://www.ncbi.nlm.nih.gov/pubmed/13302815.

90. Xiao, X., Zhao, T., Miyagishima, K. J., Chen, S., Li, W., Nadal-Nicolás, F. M., 2021: Establishing the ground squirrel as a superb model for retinal ganglion cell disorders and optic neuropathies. *Lab. Invest*., 101, 9, 1289–1303. Available at https://www.nature.com/articles/s41374-021-00637-y.

Received October 6, 2023
Accepted January 31, 2024